Journal of International Scientific Publications: Materials, Methods and Technologies

Volume 8, ISSN 1314-7269 (Online), Published at: http://www.scientific-publications.net

# OPTIC METHODS OF INVESTIGATION FOR THE TWO-PHASE FLOWS WITH HIGH CONCENTRATION OF THE DISPERSED PHASE

Aleksey R. Evseev

Federal State Budget Research Institution Kutateladze Institute of Thermophysics

Siberian Branch of the Russian Academy of Sciences, Lavrentiev's ave. 1, Novosibirsk, 630090

**Abstract**

*This study deals with development and application of the optic methods for investigation of the two-phase flows with high concentration of dispersed phase (optically opaque). The original three-fiber optical probe of the laser Doppler anemometer (LDA), operating in the regime of back-scattering, was developed. The velocities and concentrations of particles in a circulating fluidized bed were measured. The modified two-fiber optic probe of the reflecting type was developed; this sensor was used for measurements of the liquid film thickness inside the distillation column. The field of its application includes high-concentrated two-phase flows, difficult-to-reach places (behind an obstacle), and full-scale objects. The method of refractive index matching (RIM) was developed for investigation of the highly concentrated solid-liquid flows. The turbulent regime of liquid filtering inside the flow passage of the regular packed bed was investigated with application of LDA and RIM technique.*

**Key words:** *two-phase flows, dispersed phase, concentration, optic methods, fiber optical probe*

## 1 INTRODUCTION

The two-phase flows of gas (liquid) – solid particle type and gas-liquid flows are widely spread in nature and modern technologies. In nature they are tornados, sandstorms, raging mountain rivers, etc. Among technologies we should note the coal-dust burners, heat boilers with fluidized and circulating fluidized bed, chemical reactors with catalyst, distillation columns, etc.

At high concentrations of dispersed phase (above ~ 3%) these flows become optically opaque and their diagnostics by traditional optic methods is restricted or even impossible (Dubnistchev et al. 1975; Protasov et al. 2006). In (Protasov et al. 2006; Varaksin et al. 2001; Varaksin et al. 1996) they consider peculiarities of measurement of the large particle velocity in dusty flows by means of the standard Laser Doppler Anemometer (LDA) on the basis of traditional optics and the methods of amplitude discrimination and measurement of mass concentration of particles; restrictions for the LDA methods depending on the width of the two-phase flow, its concentration and particle size are determined there. To perform measurements in the two-phase flows with high concentration of dispersed phase, the optic head of LDA was modernized in (Werther et al. 1996; Wei et al. 1998), and this expands the range of dispersed phase concentration of up to 20% and higher.

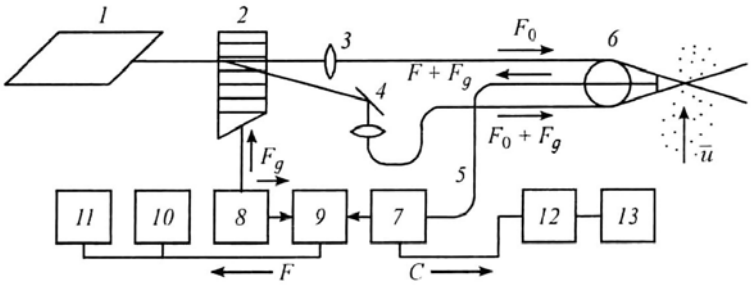
To study the local characteristics in the two-phase flows, different fiber-optic sensors are often applied; theses sensors have some advantages: small (~ 125 μm) diameter; high elasticity and mechanical strength; high corrosion resistance, wide frequency band and insignificant losses. In these sensors the optic fiber can be used both as a transmission line and as a sensitive element.

In our work we consider one-, two- and three-fiber optic sensors. On the basis of these sensors the differential and inverse-differential schemes of the laser Doppler anemometer (LDFA-3) as well as the LDFA-1 scheme with the reference beam were implemented. In these schemes the light guides serve as the units of forming and receiving LDA optics. The modified two-fiber sensor, which allows the measurement for the liquid film thickness in hard-to-reach places and at the field objects, was developed. The use of fiber-optic sensors for investigation of local characteristics in the two-phase flows with high concentration of dispersed phase showed their efficient operation until the achievement of maximal packing of solid particles and bubbles in the gas-liquid flows (Evseev, 2013).

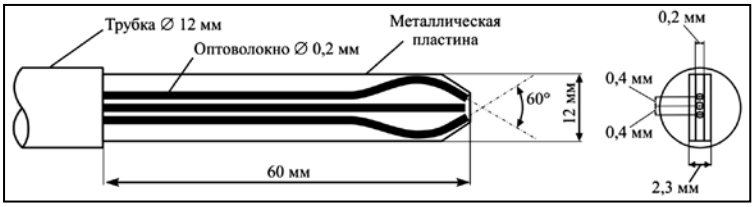
The method of optic uniformity with accurate adjustment of refraction index for special immersion liquid and dispersed glass particles was developed for the liquid flows with solid particles. Such a two-phase medium is optically transparent in a wide range of dispersed phase concentration and acceptable for investigation of a local structure by such optic methods as LDA, PIV, PTV, etc. (Evseev, 2013; Volkov et al. 1980; Romanov, 1988; Yevseyev et al. 1991).

## 2 DEVELOPMENT AND APPLICATION OF THE THREE-FIBER SENSOR OF LASER DOPPLER ANEMOMETER OF DIFFERENTIAL AND INVERSR-FIFFERENTIAL TYPE

To study hydrodynamics of different optically opaque dispersed systems such as fluidized and circulating fluidized beds, high-concentration gas-liquid flows and other, the LDFA scheme with three fibers (LDFA-3) was developed (Evseev, 2013; Evseev&Orlov, 1986; Evseev&Nakoryakov, 1982; Evseev et al. 1997). In this scheme flow probing is carried out by two crossing beams. It is similar to the differential scheme with back scattering, well-known in laser anemometry.




(a)




(b)

Fig. 1 a, b. The flowchart of three-fiber LDFA-3 with the Bragg cell (a) and concentration of the three-fiber sensor of differential type (b).

The principle scheme of LDFA-3 with three fibers is shown in Fig. 1a. The fibers serve as the units of forming and receiving optics. The beam of He - Ne laser 1 (power of 15 mW, $\lambda$= 632.8 nm is the length of radiation wave) is split by Bragg cell (20 MHz) into two beams of equal intensity. By means of microobjectives 3 they are introduced into the forming fiber of the multimode (or single-mode) type, 4-turn prism. At the outlet of forming fibers the light beams are superposed spatially in the studied range by means of rigid fixation of the fiber tips in special grooves of the plate 6, made in accordance with geometry of the differential scheme (Fig. 1 b). The directing grooves set the crossing angle (60º) for two probing beams in the measurement volume, and spatial superposition of these beams forms the interference field. When particles cross the measurement volume of the sensor, amplitude modulation of scattered radiation occurs. The measurement volume of sensor was ~ 0.0435 $mm^3$, and a distance from its geometrical center to the sensor end was 0.5 mm. The multimode fiber of quartz-quartz type with aperture of ± 10° (KK/100 /120 /200 are diameters of the fiber core, reflecting cover and protection coating, μm) were used; the length of fibers in experiments was 10 m. Scattered radiation is sent to photodetector 7 through receiving fiber 5, located symmetrically relative to two forming lines. An electron signal from the photodetector passes through the filters of the lower and upper frequencies and it is sent to mixer 9, a signal from the main generator 8 (20 MHz) is also sent to this mixer. A Doppler signal distinguished by the mixer is measured by a special processor of the tracking type 10 and observed at oscillograph 11. An electron signal from the photodetector is also sent to comparator 12, whose outlet is connected to the frequency meter 13, for measuring particle concentration. Particle concentration in the two-phase flow was measured by the time of their stay in the measurement volume of the sensor during given observation period *T*, according to algorithm $\varphi_t = \sum t_i / T$, where $t_i$ is time of the *i*-th particle stay in the measurement volume of the sensor, the measurement error was ± (10-15)%.

Operation of the differential scheme of velocity meter with the fibers is determined by the following parameters: angle between the forming fibers, aperture of optic fibers and distance between the outlet ends of the fibers. According to analysis of operation of the three-fiber scheme [11], the minimal methodic error caused by divergence of laser beams, which form the measurement volume of LDFA-3, is achieved at high crossing angles (50-70)°, where is does not exceed 10% (Fig. 2 a, b).

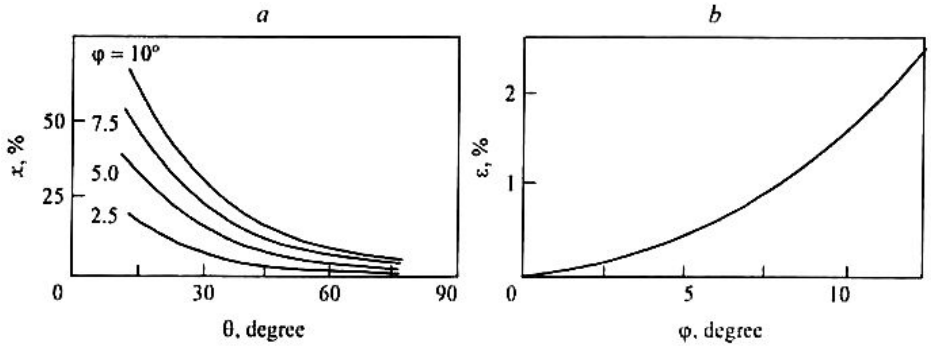
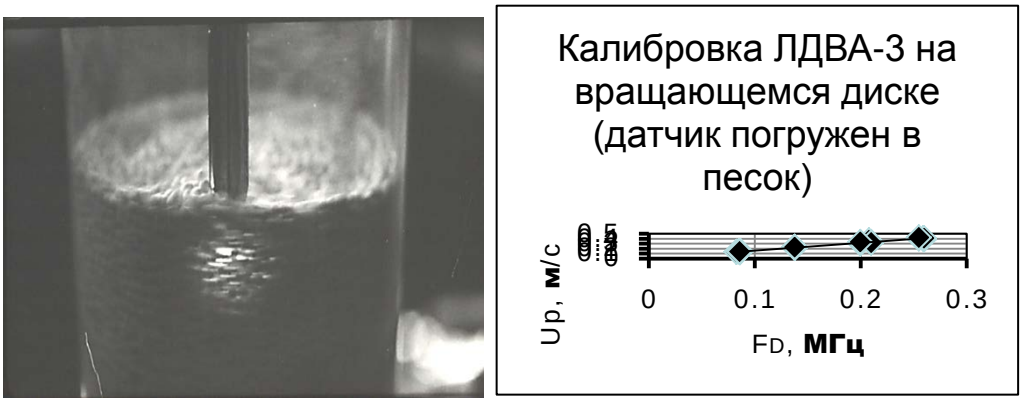



Fig. 2 a, b. (a) Dependence of methodical errors of frequency measurements of Doppler signal χ on the angle of probing beams crossing (θ), and fiber aperture (b) (Evseev&Orlov, 1986).

Operation of LDFA-3 sensor at high concentration of dispersed phase was checked in experiments with a rotating disc, where a glass cylindrical vessel of 200-mm diameter and 100-mm length filled with sand with the average grain size of $d_p$= 0.5 mm was mounted (in the center of the disc). The LDFA-3 sensor was immersed into sand to the depth of about 20 mm at a given distance from the disc center (Fig. 3 a). At disc rotation with a given velocity the Doppler frequency shift ($F_D$), scattered by liquid particles, was measured. The calibration measurements showed that an error of particle velocity measurement at high concentration (~ 50%) did not exceed 10% (Fig. 3 b).




(a) (b)

Fig. 3 a, b. Calibration setup (a) and measurement results for the sand particle velocity on a rotating disc (b).

Velocities of aluminum oxide ($Al_2O_3$) particles with the average diameter $d_p$= 0.6 mm and density $\rho_p$= 3680 kg/m$^3$ were measured by the LDFA-3 sensor in the apparatus of 100-mm diameter at air fluidized bed. The height of filling layer of particles (Ho) was 100 mm. The gas-distributing grate was made of two perforated plates and a mesh packing between them; the mesh cell was 0.1×0.1 mm$^2$. The rate of minimal fluidized bed ($U_{mf}$ ) was 0.24 m/s. The axial and radial components of particle velocity (Fig. 4) were measured at the axis of fluidized bed (FB) apparatus at distances h/Ho=0.05, 0.65 and 0.95 from the gas-distributing grate. The operation conditions of FB apparatus were close to minimal fluidization. The values of particle velocities are shown along the abscissa axis, and probability of instantaneous velocity relative to the total number of measurements is shown along the ordinate axis. Measurement results show that at $h/H_0$=0.65-0.95 the fluidized bed is in the state of intensive mixing. However, near the gas-distributing grate ($h/H_0$=0.05) probability of high

velocities decrease significantly, and this is caused by a smaller size of bubbles in this area. The maximal velocity of particle motion relates to the velocity of bubble motion, determined by their size. Therefore, dispersed phase velocity and concentration in the high-concentrated two-phase flows are measured by the LDFA-3 sensor and special unit of electronic processing.

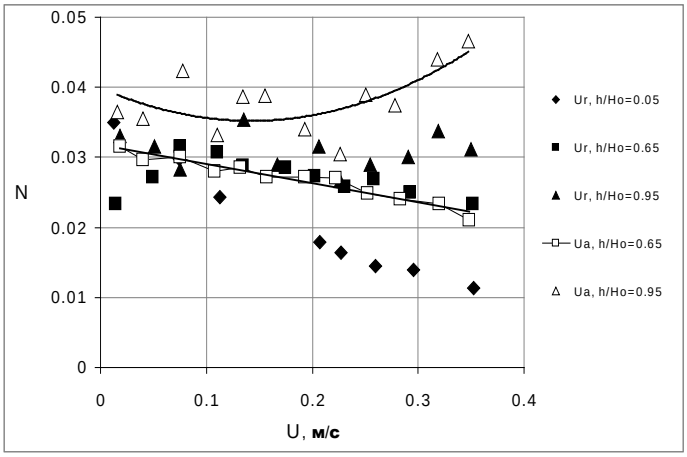



Fig. 4. Distribution of probability density of axial (Ua) and radial (Ur) particle velocity components at the axis of a laboratory setup with fluidized bed.

The flowchart of inverse-differential scheme of the laser anemometer for measuring the dispersed material velocity with the same fiber-optic sensor (Fig. 2b) is shown in Fig. 5 a, b. The beam of He-Ne laser 1 (15 mW, $\lambda$ = 632.8 nm) was sent to multimode fiber 3 by means of gradient lens 2. Receiving fibers 4 and 5 are located at angle $\pm\ \theta = 30^{o}$ relative to probing light guide 3 according to geometry of the inverse-differential scheme. After adjustment the light guides are rigidly fixed in the directing grooves of the sensor and closed from the top by a laminar lid with a thickness of 0.8 mm. A laminar sensor (Fig. 2 b) is connected to a tube-holder, which directs it to the studied area of the two-phase flow. A particle moving in the measurement volume of the sensor diffuses probing radiation, which partially comes to receiving fibers 4 and 5. Due to the Doppler effect, the frequency of the scattered light in fiber 4 has shift $F_{D1}$, and in fiber 5 this shift is $F_{D2}$. At the outlet of fibers the scattered light is sent to cube-prism 8 by gradients lenses (2), where their spatial superposition occurs.

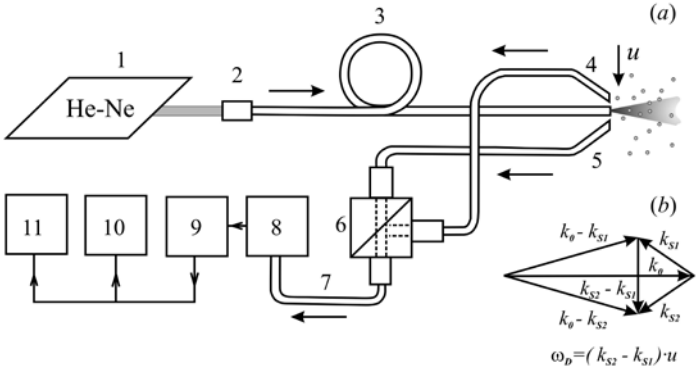



Fig. 5 a, b. Inverse-differential scheme of the laser Doppler anemometer (LDFA-3) with fiber-optic sensor (a), and geometry of optic beams (b).

A signal of difference Doppler frequency $F_D = (F_{D1} - F_{D2})$ is fed through gradient lens of 1.5-mm diameter 9 to fiber-optic module 10, and then to photodetector 11. The photocurrent pulses, modulated by difference Doppler frequency, after filters of low and high frequencies 12 are sent to the tracking processor 13 and spectrum analyzer 14 for analysis and processing. The velocity of particle motion is determined by the known expression

$U \cdot \cos\alpha = F_D \lambda/2\sin\theta$, where $U \cdot \cos\alpha$ is projection of velocity vector on the direction of vertical difference vector of the scattered beams (Fig. 5 b). The inverse-differential scheme is easily converted into the differential LDA scheme, and this significantly simplifies the adjustment of the fiber-optic sensor.

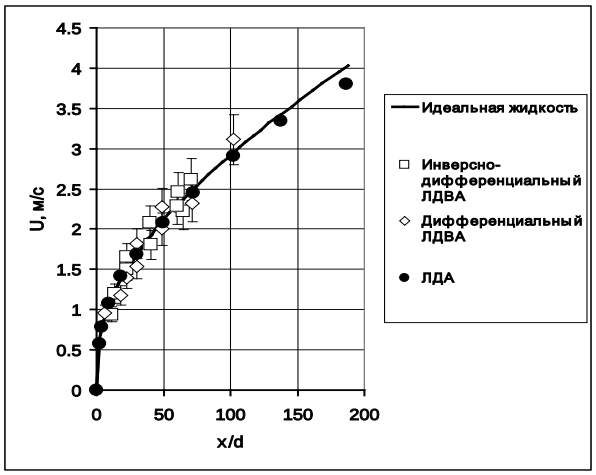



Fig. 6. Calibration measurements of particle velocity at gravitation deposition of sand jet flowing from a cone.

The velocity of sand particles with the average size of 0.5 mm and density of 2620 kg/m$^3$ was measured at gravitation deposition of the jet, flowing from a hole (d=4.7 mm) of a cone with total angle of 30º. The fiber-optic sensor worked in the framework of both LDFA inverse-differential scheme and differential scheme (Fig. 6). Dimensionless height from the cone hole (h/d) is shown along the abscissa axis and velocity of sand particles deposition at the axis of gravitation jet is shown along the ordinate axis. Previously it was shown that the velocity of particles at the jet axis corresponds to the velocity of ideal liquid flowing from a hole (Evseev, 1994). According to the measurements, the ratio of a signal to noise is the same for both schemes. However, the energy level of a signal in the LDFA differential scheme is two times higher.

## 3 DEVELOPMENT AND APPLICATION OF THE ONE-AND TWO-FIBER SENSOR FOR MEASURING CHARACTERISTICS OF THE TWO-PHASE FLOWS AT HIGH CONCENTRATION OF DISPERSED PHASE

The laser Doppler anemometer with one light guide (LDFA-1) was used to measure the velocity of cryolite particle motion in the sedimentation apparatus with inclined walls and velocity of gas phase (“slug”) emersion in the gas-uplift setup with the diameter of 15 or 16 mm and length of (l) 6.0 or 2.7 m. The beam of He-Ne laser I (power of 15 mW, λ= 632.8 nm) passes through the hole in inclined mirror 2 and it is introduced into fiber 4 by microobjective 3. The fiber sends probing radiation into studied two-phase medium 5 in the form of a cone with vertex angle ~ (15-20)°. The plane of laser beam polarization fluctuates chaotically, and speckles are observed in the cone cross-section. The role of reference beam in this scheme is played by the wave reflected from the outlet end of the fiber, which relates to the difference of refractive index of liquid and fiber. When a bubble or particle approaches the end, the scattered (reflected) light comes partially to the fiber and together with the reference wave it is sent to mirror 2 in the reverse direction. After reflection from the mirror the beams pass through polarization filter 6, whose transmission plane is orthogonal to the plane of laser beam polarization. Then, both beams are sent by objective 7 to diaphragm 8 and photodetector 9. Beam interference leads to high-frequency modulation of the outlet current of the photodetector. Thus, the considered scheme is similar by the operation principle to the scheme with reference beam of an ordinary LDA, operating under the conditions of reverse scattering, where the fiber serves as the forming and receiving optics. The electronic part of the measurement system includes the standard set of equipment of the ordinary LDA: photodetector 9, filter of low and high frequencies 10, spectrum analyzer 11, unit of Doppler signal processing 12. Dispersed phase concentration is measured as in the differential scheme of LDFA-3. For this purpose, an electronic signal is sent to low frequency filter 13, comparator 14 and frequency meter 15. The connection between a projection of interface velocity on

the fiber axis and measured Doppler frequency $F_D$ is determined by known expression $U \cos\alpha = F_D \lambda/2n_f$ (Lisizin et al. 1980, Evseev, 1982), where $n_f$ is refractive index of the studied medium.

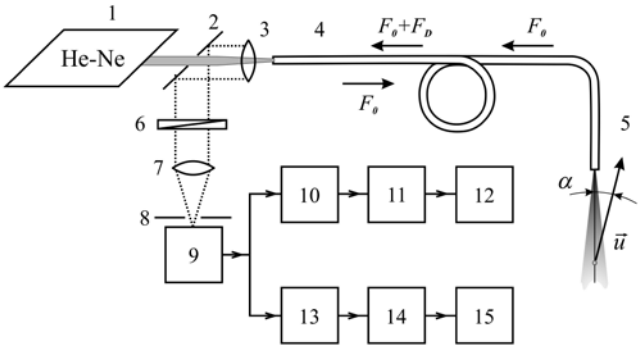
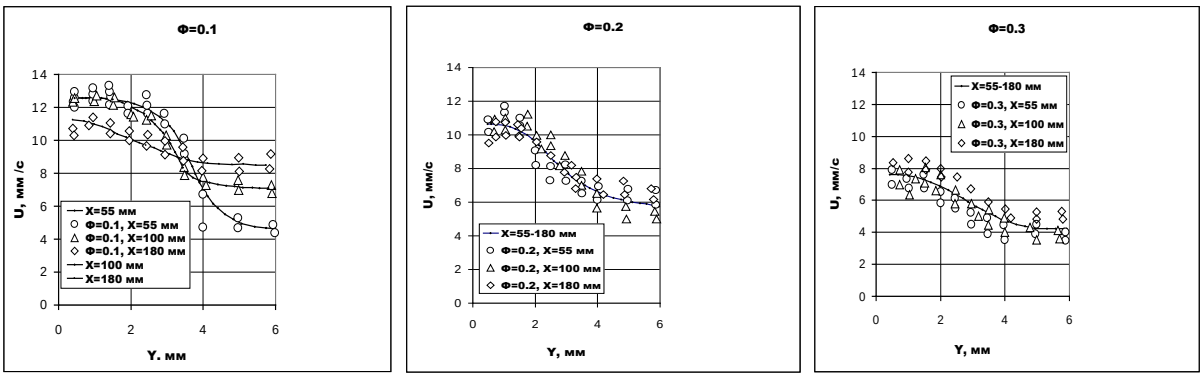



Fig. 7. The flowchart of one-fiber LDFA-1 for measurement of dispersed phase velocity and concentration in the two-phase flows.

Results of investigation of the processes of consolidated deposition of cryolite ($d_p$=40 μm, $\rho_p$= 3000 kg/m$^3$), performed in the sedimentation setup with a cross-section of 0.15×0.1 m$^2$ and height of 0.5 m, with the angle of inclination of $60^0$ are shown as an example. The velocity of particle motion was measured in three cross-sections of a boundary layer under the upper (plate on top) channel wall at distances X=55, 100 and 180 mm from its bottom. Weight concentration (Φ) of cryolite in experiments was 0.10, 0.20 and 0.30 (Evseev et al. 1984). At deposition of the main part of cryolite, a convective upflow of clean (clarified) liquid is formed in a thin boundary layer (~ 2 mm) under the upper wall of setup. At that, the velocity of cryolite deposition increases almost by ~ 43%. A transitional area with the thickness of about 4 mm is observed between the counter-current flows; particle concentration in this area changes from zero to average concentration in the setup.

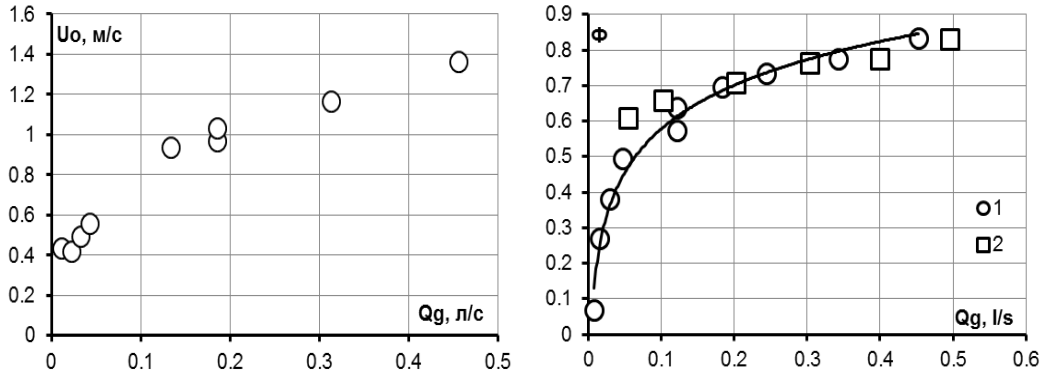



(a) (b) (c)

Fig. 8 a, b, c. The profiles of cryolite particle velocity (“ceiling” plate) at deposition in the sedimentation setup with inclined walls (Evseev et al. 1984).

The profiles of average velocities in the flow of clarified liquid under the upper wall of the channel are shown in Fig. 8 a-c for three cross-sections along the channel at mass concentration of cryolite of 0.10, 0.20 and 0.30. With a rise of cryolite concentration within the mentioned limits the velocity of liquid in the zone of boundary layer with the thickness of ~ (0.5-2.0) mm decreases gradually by ~ (35-40) %. All velocity profiles have a bend point, and this proves intensive vortex motions in the transitional zone between the counter flows. The velocity profiles do not change along the wall, excluding the area near the liquid-particle interface. Similarity of velocity profiles and their dependence on cryolite concentration are observed in experiments. With an increase in mass concentration of a solid

phase we can observe a relative decrease in the velocity of particle motion. Not only velocity difference between the outer and inner parts of the layer changes, but also the absolute value of velocity in its inner part.




(a) (b)

Fig. 9 a, b. Gas phase velocity (a) and concentration (b) at gas-uplift at the tube axis depending on the gas flow rate: 1- d=16 mm, L=2.7 m; 2- d=15 mm, L=6.0 m.

Dependences of velocity ($U_0$) and gas phase concentration (Φ) at the axis of a vertical tube (gas-uplift regime) on gas flow rate are shown as an example of LDFA-1 application in Fig. 9 a, b. The measurements were carried out in the tube with 16-mm diameter and 2.7-m length as well as in the tube with 15-mm diameter and 6.0-m length. The features of interaction between the fiber sensor tip and bubbles and peculiarities of LDFA-1 operation in the gas-liquid flow are presented in (Evseev, 1982; Evseev et al. 1987). At an increase in the flow rate the growth of gas phase velocity and almost exponential increase in its concentration are observed. At that, productivity of gas-uplift by water lifting increases also. The efficiency of gas-uplift under the conditions of bubble flow of the gas-liquid mixture is higher than that in the slug flow. At an increase in the gas flow rate bubble concentration increases; they merge into the slugs at Φ > 30-40%. With a change in the flow of the gas-liquid mixture the relative efficiency of the gas-uplift decreases.

## 4 THE MEASUREMENT OF LIQUID FILM THICKNESS

Small distances (~1-3 mm) to a reflecting surface (e.g., water surface) can be measured by means of the LDFA-1 sensor by the analogy with a reflective type sensor. The measurement method for the liquid film thickness is based on illumination of a reflecting surface by the divergent light beam at the outlet of probing light guide and registration of intensity of reflected light at calibration at a given distance. The thickness of liquid nitrogen film on a vertical plane of 250×75×5 mm was measured in the range of flow rates from 0.5 $cm^3/s$ to 4 $cm^3/s$ under the conditions of cryogenic temperatures (Alekseenko et al. 2003). The Reynolds number in experiments was changed from 30 to 280. Liquid nitrogen flew from the constant header tank through a distributing slot to the plate inside the cryostat. A single-fiber sensor (LDFA-1) was mounted flush in a bush at distance of 190 mm from the front plate edge. Dependence of dimensionless film thickness $h_d$ on Re number is shown in Fig. 10. Here $h_d = 4g^{0.5}h^{1.5}/\nu_1$ , g is free fall acceleration, $\nu_1$ is kinematic viscosity of liquid nitrogen, ▲ shows data of LDFA-1 for liquid nitrogen (Alekseenko et al. 2003), (○) are data for Gimbutis water (Gimbutis, 1988), (*) are data for liquid nitrogen (Pavlenko et al. 1995). Coincidence of these results can be considered satisfactory.

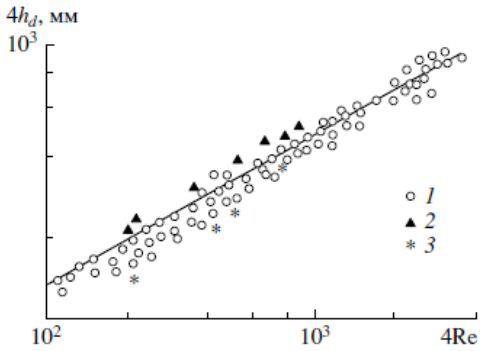



Fig. 10. Dependence of dimensionless film thickness $h_d$ on Reynolds number (Alekseenko et al. 2003).

The scheme of LDFA-1 can be simplified, if instead of the directional coupler (mirror) we use the parallel ends of two fiber with a glued glass plate with the thickness of about 1-2 mm (Evseev, 1997). The beam of He-Ne laser 1 is introduced into probing sensor 3 by means of gradient lens 2 (Fig. 11).

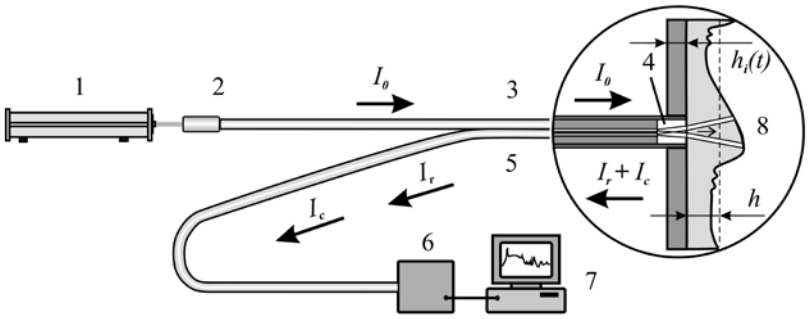



Fig. 11. The flowcharts for measurements of the liquid film thickness by modified two-fiber sensor.

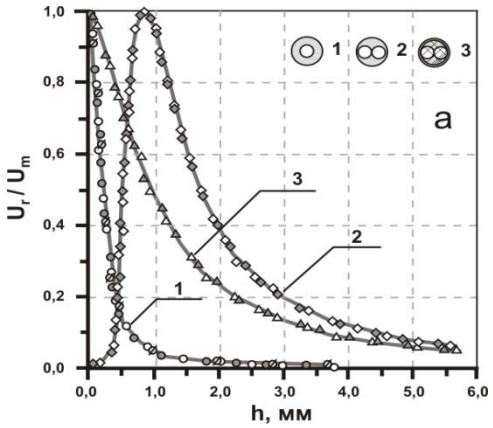



Fig. 12. Dependence of the relative stress of fiber sensors on the distance to the reflecting surface of glass: (1) – one-fiber; (2) two-fiber; (3) – modified two-fiber probe.

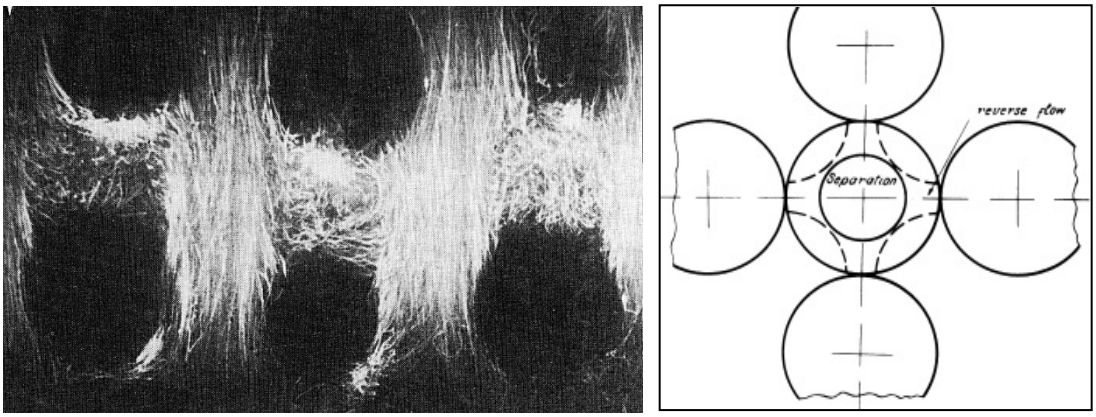
This modified two-fiber probe can be used for the measurement of the liquid film thickness as well as dispersed phase velocity and concentration in concentrated two-phase flows. The dispersed phase velocity can be measured by the Doppler frequency shift in the light scattered by particles (by the analogy with LDFA-1), and dispersed phase concentration can be measured by the analogy with the reflective type sensors.

The measurement method for amplitude-frequency characteristics of the liquid film thickness in hard-to-reach places and on the objects with complex configuration was developed on the basis of modified two-fiber probe.

The modified fiber-optic sensor for the measurement of liquid film thickness has some advantages over other probes: high operation speed ($10^{-4}$÷$10^{-5}$s), low area of film surface probing (~ 0.12 mm$^2$), high measurement accuracy (1.5-2% for smooth films, 10% for wavy films) and long flow line between an object and device (more than 100 m). The use of a modified two-fiber sensor for investigation of the mechanism of liquid spreading at the counter air flow in the distillation column with the packing of corrugated sheets is shown in (Alekseenko et al. 2008) and measurement of the liquid film thickness with a local heater is shown in (Zaitsev et al. 2003).

## 5 INVESTIGATION OF LOCAL CHARACTERISTICS OF THE TURBULENT FILTRATIONAL FLOW WITH APPLICATION OF LDA AND RIM TECHNIQUE

Coincidence of refractive index of liquid and glass balls ensures optic uniformity of the system and possibility of measurements at any point of the turbulent filtration flow with the help of LDA "LADO-2". On the basis of visual observations (Fig. 13 a) and investigation of local characteristics the physical model of the turbulent filtration flow in the cubic packing was developed (Fig. 13 b); it includes the jet zone in the cell center, detachment (vortex) zone in the area of a shadow contact point, and zones of reverse flow, directed to the lateral contact points of the balls. Three components of the average liquid velocity and RMS pulsations were measured in the mentioned zones as well as the spectrum of longitudinal pulsations in the jet zone and mixing layer (Evseev et al. 1991). The Reynolds number in experiments was changed from 1000 to 20000.




(a) (b)

Fig. 13 a, b. Turbulent filtration flow in the cubic packing of balls at Re= 500 (a), and its physical model (b).

The profiles of three components of average velocity (a) and RMS pulsations (b) in a minimal cross-section of a cubic cell are shown in Fig. 14 a, b. The ball diameter (D=18 mm) and maximal flow velocity $U_m$ in a cell were taken as the length and velocity scales. The jet is formed in this cross-section of a cell ($S_{min}$), then, it expands in the diffuser part ($S_{dif}$) to the plane passing through a shadow point of balls contact ($S_{max}$). Then, the jet flows to the confusor part of a cell ($S_{conf}$), where it is constricted to the initial state ($S_{min}$). The relative longitudinal velocity at the axis in a cubic cell and its RMS pulsations change in the following manner: $U/U_m$= 1, $\sigma_u \approx$ (9-10)% in cross-section 1 ($S_{min}$); $U/U_m \approx 0.9$, $\sigma_u \approx$ (12-13)% in cross-section 2 ($S_{dif}$); $U/U_m \approx$ 0.75-0.8, $\sigma_u \approx$ (15-16)% in cross-section 3 ($S_{max}$); $U/U_m \approx 0.9$, $\sigma_u \approx$ (12-13)% in cross-section 4 ($S_{conf}$). Cross-sections 1-4 are located along the flow at distance D/4. The cross and transversal components of liquid velocity at the jet axis are zero (due to flow symmetry), and RMS pulsations are almost equal to the longitudinal ones. At the cell periphery in the shadow area of the ball there is the zone of reverse flow, where the flow divided into four branches passes to the lateral contact points: $U/U_m \approx 0$, $\sigma_u \approx 0$ in cross-section 1; $U/U_m \approx$ -(0.06-0.07), $\sigma_u \approx$ (5-6)% in cross-section 2; $U/U_m \approx$ -(0.12-0.13), $\sigma_u \approx$ (10-12)% in cross-section 3. In the confusor part of a cell (cross-section 4) there is no reverse flow because of acceleration of the filtration flow.

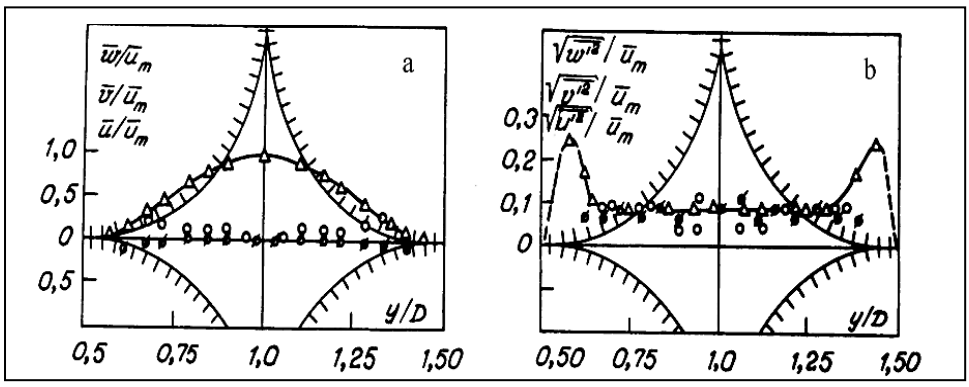



Fig. 14 a, b. Profiles of three components of the average velocity of filtration flow (a) and RMS pulsations (b) in the minimal cross-section of a cubic cell at Re=17400

(Yevseyev et al. 1991).

The cross velocity component of liquid in the zone of reverse flow is close to zero and the transversal component varies in the same limits as the longitudinal component. Pulsation intensities of all three components of the flow velocity in the zone of reverse flow are almost equal. In the mixing layer between the jet area and zone of reverse flow RMS pulsations of all three velocity components are maximal and almost equal, excluding zone of ~1-2 mm near the lateral contact points of balls: $\sigma_u \approx$ (24-28)%, $\sigma_v = \sigma_w \approx 0$ (cross-section 1); $\sigma_u = \sigma_v = \sigma_w \approx$ (22-23)% in cross-section 2; $\sigma_u = \sigma_v = \sigma_w \approx$ (19-20)% in cross-section 3.

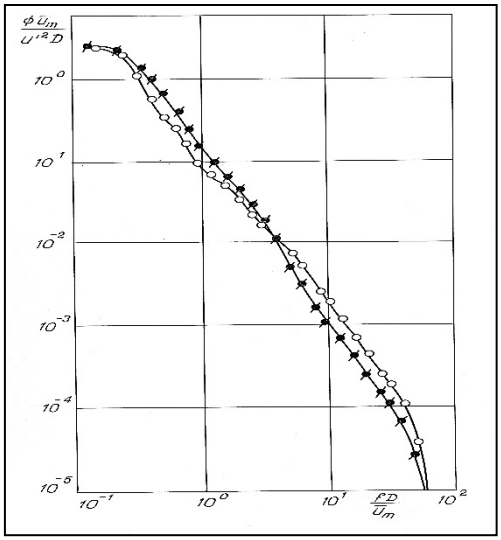


Fig. 15. The normalized spectrum of pulsations of the longitudinal velocity of filtration flow in diffuser cross-section 2 at cell axis and at the boundary of reverse zone (○) at Re=$1.74 \times 10^4$ (Yevseyev et al. 1991).

The spectral characteristics of longitudinal velocity pulsations were studied in cross-section 2 at the jet axis and in the mixing layer of filtration flow оси струи (Fig. 15). In contrast to the known Kolmogorov's law of "–5/3", the spectral function decreases inversely proportional to the square of the wave number. In the spectrum of velocity pulsations there are no discrete components and the maximal scale of pulsations has the order of the ball diameter.

## CONCLUSIONS

1. Experimental investigation of the two-phase flows at high concentrations of dispersed phase is impeded by optical opaqueness, excluding the case of optical uniformity of the flow with the same refractive index of both phases. The fiber-optic sensors disturb the two-phase flow, require calibration and corrections. However, they are relatively easy for experimental use and do not require high costs.

2. The method for measuring particle velocity (with the error of 10-15 %) and concentration in the turbulent two-phase flows with high concentration of dispersed phase was developed on the basis of LDFA-3 as well as the original design of the sensor.

3. The method for measuring particle and bubble velocity (with the error of 10 %) and concentration in the gas-liquid flows by means of LDFA-1 was developed together with the sensor design.

4. The method for measuring the liquid film thickness (with an error of 10 %) by means of the two-fiber modified sensor was developed. The effective design of sensor for the measurements in hard-to-reach places and at the field objects was worked up.

## REFERENCES

Alekseenko S.V., Markovich D.M., Evseev A.R. et al., 2008. Experimental investigations of liquid distribution over the spructured packing, AIChE J., V. 54, No. 6, P. 1424-1430.

Alekseenko S.V., Bobylev A.V., Evseev A.R., Markovich D.M. et al., 2003. Measurements of the liquid-film thickness by a fiber-optic probe, Instruments and Experimental Techniques, No. 2, P. 260-264.

Dubnischev Yu.N., Evseev A.R., Sobolev V.S.,Utkin E.N., 1975. Study of gas-saturated turbulent streams using a laser doppler velocity meter. J. Appl. Mech. Techn. Phys., No. 1, P. 114-119.

Gimbutis G., 1988. Heat transfer of a falling fluid film. Vilnius: Mokslas, 233 p.

Evseev A.R., 2013. Experimental Investigation of a Local Structure of Turbulent Two-Phase Flows with High Concentration of Dispersed Phase. Doctoral Dissertation, Kutateladze Institute of Thermophysics SB RAS, Novosibirsk, 299 p.

Evseev A.R., 1997a. Liquid film thickness measurement by the fiber optical probe, Proc. Int. Symp. on the Physics of Heat Transfer in Boiling and Condensation, Moscow, Russia, P. 519-523.

Evseev A.R., Orlov V.A., Ryabov G.A., 1997b. Measurements of velocity and concentration of particles in circulating fluidised bed by differential Doppler anemometer with fiber optics. Proc.of the 7-th Int. Conf. on Lazer Anemometry. Sept. 8-11, Karlsruhe, Germany.

Evseev A.R., 1994. Measurement of Turbulent Characteristics of a Two-Phase Gravitation Jet, Rus. J. Engineering Thermophysics, V. 4, No., P. 313-322.

Yevseyev, A.R., Nakoryakov, V.E. & Romanov, N.N., 1991. Experimental investigation of a turbulent filtrational flow. Int. J. Multiphase Flows, V. 17, No. 1, P. 103-118.

Evseev A.R., Nakoryakov V.E., Pokusaev B.G., Tachkov S.A., Timkin L.S., 1987. Measurement of structure characteristics of the gas-liquid flow by the laser anemometer with a fiber light guide, Optoelectronics, Instrumentation and Data Processing, No. 2, P. 69-73.

Evseev A.R., Orlov V.A., 1986. Differential Doppler velocity meter with fiber light guides. Optoelectronics, Instrumentation and Data Processing, No. 6, P. 62-68.

Evseev A.R., Zaostrovsky P.F., Pospelov F.M., Uspensky M.S., 1984, Hydrodynamics of inclined channel of a laminar settler by the laser anemometer with a fiber-optic path. Theor.Found.Chem. Engn, Vol. 23, No. 3, P.407-410.

Evseev A.R., Nakoryakov V.E., 1982. Laser Doppler anemometer for investigation of fluidized bed structure. In book: Transfer Processes in High-Temperature and Chemical Reacting Flows, IT SB AS USSR, Novosibirsk, P. 91-98.

Evseev A.R., 1982. Laser Doppler velocity meter with a light guide. Optoelectronics, Instrumentation and Data Processing, No. 3, P. 109-111.

Lisitsin V.N., Orlov V.A., Fomin Yu.N., Chebotaev V.P., 1980. Laser Doppler velocity meter for opaque flows of liquid and particles. In: Proc. III All-Union Conference "Experimental methods and equipment for investigation of turbulence", IT SB AS USSR, Novosibirsk.

Pavlenko A.N., Serov A.F., Chehovich V.Yu. et al., 1995. // ASME Forum on Measurement Techniques in Multiphase Flows, San Francisco, Nov., USA.

Protasov M.V., Varaksin A.Yu., Ivanov T.F., Polyakov A.F., 2006, Analysis of the possibility of using laser Doppler anemometer for the investigation of highly dust-laden flows. High Temperature, Vol. 44, No. 2, P. 296-301.

Romanov N.N., 1988. Turbulent Characteristics of the Flow in Regular Ball Packing. Candidate Dissertation, Kutateladze Institute of Thermophysics SB RAS, Novosibirsk, 187 p.

Varaksin A.Yu., Ivanov T.F., Polyakov A.F., 2001. Laser Doppler anemometer measurement of large-particle relative concentrations, Measurement Techniques, No 8, P. 852-856.

Varaksin A.Yu., Полежаев Ю.В., Polyakov A.F., 1996. Efficiency of amplitude selection of signals in a study of heterogeneous flows using a laser-doppler anemometer, Measurement Techniques, No. 6, P. 645-651.

Volkov V.I., Mukhin V.A., Nakoryakov V.E. et al., 1980. Hydrodynamics of the wall layer in a cubic-packing model. J. Appl. Mech. Techn. Phys., No.6, P.786-789.

Wei F., Lin H., Cheng Y., Wang Z., Jin Y., 1998. Profiles of particle velosity and solids fraction in a high-density riser. Powder Technol., V. 100, P. 183-189.

Werther J., B. Hage B., Rudnick C., 1996. A comparison of laser Doppler and single-fibre reflection probes for the measurement of the velocity of solids in a gas-solid circulating fluidized bed. Chemical Engineering and Processing, V. 35, P. 381- 391.

Zaitsev D.V., Kabov O.A., Evseev A.R., 2003. Measurement of locally heated liquid film thickness by double-fiber optical probe, Experiments in Fluids, V.34, No. 6, P. 748-754.